
# Fatigue mechanism of textured Pb(Mg1/3Nb2/3)O3-PbTiO3 ceramics

Yongke Yan, Yuan Zhou, Shashaank Gupta, and Shashank Priya

Citation: Applied Physics Letters **103**, 082906 (2013); doi: 10.1063/1.4819223
View online: http://dx.doi.org/10.1063/1.4819223
View Table of Contents: http://scitation.aip.org/content/aip/journal/apl/103/8?ver=pdfcov
Published by the AIP Publishing

# Fatigue mechanism of textured $Pb(Mg_{1/3}Nb_{2/3})O_3$-$PbTiO_3$ ceramics

Yongke Yan,[a] Yuan Zhou, Shashaank Gupta, and Shashank Priya[b]
*Bio-inspired Materials and Devices Laboratory (BMDL), Center for Energy Harvesting Materials and Systems (CEHMS), Virginia Tech, Blacksburg, Virginia 24061, USA*

(Received 1 July 2013; accepted 11 August 2013; published online 22 August 2013)

Grain orientation, $BaTiO_3$ heterogeneous template content, and electrode materials are expected to play an important role in controlling the polarization fatigue behavior of ⟨001⟩ textured $Pb(Mg_{1/3}Nb_{2/3})O_3$-$PbTiO_3$ ceramics. A comparative analysis with randomly oriented ceramics showed that ⟨001⟩ grain orientation/texture exhibits improved fatigue characteristics due to the reduced switching activation energy and high domain mobility. The hypothesis was validated from the systematic characterization of polarization—electric field behavior and domain wall density. The defect accumulation at the grain boundary and clamping effect arising from the presence of $BaTiO_3$ heterogeneous template in the final microstructure was found to be the main cause for polarization degradation in textured ceramic. © *2013 AIP Publishing LLC*.
[http://dx.doi.org/10.1063/1.4819223]

Anisotropy in elastic, dielectric, and piezoelectric properties plays an important role in tailoring the performance of piezoelectric materials as evident from the giant longitudinal piezoelectric coefficient $d_{33}$ (>2000 pC/N) and large electromechanical coupling coefficient $k_{33}$ (>90%) measured along ⟨001⟩ directions in domain engineered relaxor-ferroelectric single crystals, such as $Pb(Mg_{1/3}Nb_{2/3})O_3$-$PbTiO_3$ (PMN-PT) and $Pb(Zn_{1/3}Nb_{2/3})O_3$-$PbTiO_3$ (PZN-PT).[1] The outstanding electromechanical properties in these materials have driven the development of new generation of high-performance actuators, sensors, and piezoelectric energy harvesters.[2] However, the application of oriented PMN-PT and PZN-PT relaxor-ferroelectric single crystals has been limited owing to their high production cost, restriction on sample shape and size, and compositional heterogeneity across the ingot. In last few years, textured ceramics have emerged as an alternative for achieving superior performance similar to that of single crystals, while keeping the cost down.[3–5] Textured ceramics can be synthesized using the established tape-casting process and, thus, have flexibility in terms of the shape and size of the sample. We have demonstrated that textured (Lotgering factor, $f = 98\%$) PMN-PT ceramics exhibit outstanding piezoelectric and dielectric properties.[4]

Apart from high piezoelectric properties at low field drives, stability of electromechanical properties under cyclic stress and electric field loading is essential for the deployment of material. Systematic loss of the switchable polarization under cyclic external field is known as polarization fatigue.[6–8] Several mechanisms have been proposed in literature for explaining the fatigue behavior of a ferroelectric material including accumulation of charged defects at domain walls leading to their pinning,[9] formation of space charge layer at ferroelectric—electrode interface,[10,11] formation of micro-cracks due to residual strain,[12,13] field-driven phase transition,[14] and field-driven diffusion of electrode metal to grain boundaries.[15] Depending upon the operating conditions (temperature, external field magnitude, and frequency) and microstructure of the material, one or more of these fatigue mechanisms can play the governing role.[7]

In bulk polycrystalline ceramics, fatigue is highly dependent on the surface, interface, and grain boundary related imperfections.[7] In single crystals, the fatigue is mainly dominated by the accumulation of charged defects at domain boundaries and formation of micro-cracks due to the residual hysteretic strain.[13,16,17] Prior investigations have indicated the anisotropic nature of fatigue behavior in ferroelectric single crystals.[13,16–19] In $Pb(In_{1/2}Nb_{1/2})O_3$-$Pb(Mg_{1/3}Nb_{2/3})O_3$-$PbTiO_3$ single crystals, superior fatigue resistance was found in ⟨001⟩ orientation as compared to that along ⟨110⟩ and ⟨111⟩ directions. Polarization degradation was observed to suddenly occur above 50–100 bipolar cycles in ⟨110⟩ oriented samples, while ⟨001⟩ oriented samples exhibited fatigue-free characteristics up to $10^5$ bipolar cycles.[16] Thus, one can expect that grain textured ceramics will also exhibit different fatigue behavior as compared to their random counterpart. Textured ceramics can be considered as a composite of oriented matrix grains and aligned template microcrystals.[4] Thus, the change in polarization switching under continuous field cycling could be resultant of interaction between the grains and the embedded microcrystals. Naturally, the question that immediately comes to mind is "What mechanism plays the dominant role in controlling the fatigue behavior of this composite microstructure?" Very few studies have been conducted on the fatigue behavior of textured piezoelectric ceramics and, thus, this question has not been addressed. In this letter, we provide deterministic results on the effect of orientation, heterogeneous template content, and electrode layer on the polarization fatigue behavior of ⟨001⟩ textured PMN-PT ceramics.

Textured $0.675Pb(Mg_{1/3}Nb_{2/3})O_3$-$0.325PbTiO_3$ (PMN-PT) ceramic samples were synthesized by templated grain growth (TGG) process using $x$ vol. % of $BaTiO_3$ (BT) templates, abbreviated as PMN-PT-$x$BT ($x = 0$, 1, 3, 5). The TGG texturing process, synthesis of BT templates, phase and microstructure characterization have been described in detail elsewhere.[20] To conduct the electrical fatigue experiment, an AC electric field with a triangular bipolar wave form was

[a]Electronic mail: yanthu@gmail.com
[b]Electronic mail: spriya@vt.edu

 

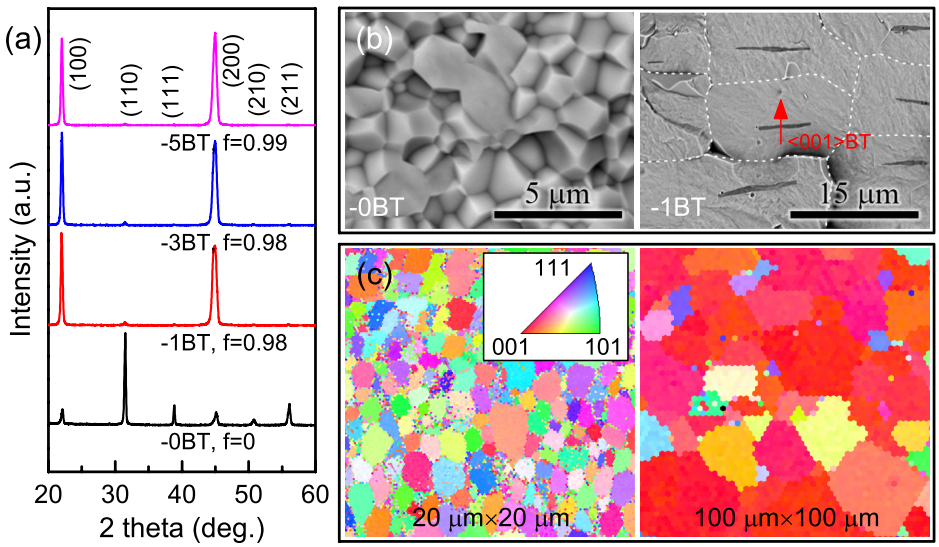


FIG. 1. (a) XRD patterns of PMN-PT-*x*BT samples; (b) cross-sectional SEM images of PMN-PT-0BT (left) and PMN-PT-1BT (right); (c) EBSD images of PMN-PT-0BT (left) and PMN-PT-1BT (right) surfaces.

applied at a frequency of 10 Hz. Impedance spectrum was measured using HP4194A over frequencies from 100 Hz to 15 MHz in the temperature range of 25 °C to 500 °C.

Figure 1(a) shows the XRD patterns of PMN-PT-*x*BT samples. Here, PMN-PT-0BT represents the random ceramic without BT seeds ($x=0$), and PMN-PT-*x*BT ($x=1,\ 3,\ 5$) represents the textured ceramics with different BT template content. X-ray diffraction (XRD) patterns confirmed the formation of perovskite structure without any noticeable secondary phase. Domination of intensities of (00*l*) peaks in PMN-PT-*x*BT ($x=1,\ 3,\ 5$) samples indicates high ⟨001⟩ orientation. Lotgering factor calculated for these samples were found to be almost same ($f>98\%$). Fig. 1(b) displays the scanning electron microscopy (SEM) images of random and textured cross-sectional samples. Compared to the equiaxed grains in random ceramics (left), all the matrix grains in textured sample (right) were well aligned with brick-wall microstructure. Another feature of textured ceramics is the existence of aligned plate-like BT template inside the oriented PMN-PT matrix. The BT template microcrystals had length of $5\sim10\ \mu$m and thickness of $0.5\sim1\ \mu$m. Therefore, besides large grain size, the textured ceramics had two other unique characteristics: ⟨001⟩ grain orientation and the existence of heterogeneous BT "core". Figure 1(c) shows the EBSD inverse pole figures of the random ceramic and textured ceramic clearly illustrating that the textured grains have strong ⟨001⟩-preferred orientation.

Figure 2(a) shows the variation of saturation polarization ($P_{max}$), remnant polarization ($P_r$), and coercive electric field ($E_c$) values as a function of number of cycles for random PMN-PT-0BT and ⟨001⟩ textured PMN-PT-5BT ceramic at 10 Hz with silver electrodes. The amplitude of the applied alternating triangular electric field was 18 kV cm$^{-1}$, which is about 3 times of coercive field ($E_c\sim6$ kV cm$^{-1}$). Both samples show the presence of typical three stages of the fatigue behavior. In the first stage, both samples show a

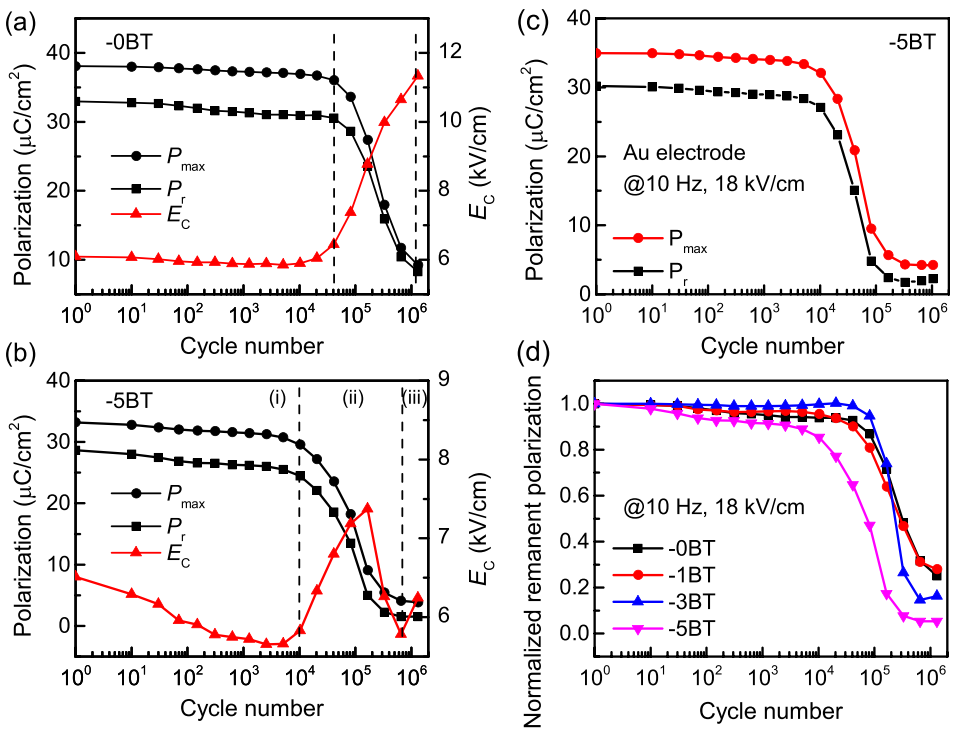


FIG. 2. Polarization ($P_{max}$), remnant polarization ($P_r$), and coercive electric field ($E_c$) as a function of number of cycles for (a) PMN-PT-0BT random ceramic and (b) PMN-PT-5BT textured ceramic at a field magnitude of 18 kV cm$^{-1}$ and 10 Hz. (c) $P_{max}$ and $P_r$ as a function of number of cycles for PMN-PT-5BT ceramic using gold (Au) electrodes; (d) normalized remanant polarization as a function of cycling number in PMN-PT-*x*BT textured ceramics.

slow degradation of polarization with electric cycling, which lasts for about $3 \times 10^4$ and $1 \times 10^4$ cycles, respectively, for random and textured ceramics. Second stage is characterized by logarithmic drop of polarization. Finally, in the third stage, both samples show saturation with very small values of polarization persisting. The functional form that has been used to analyze the relaxation in PMN-PT single crystals is a stretched exponential that is superimposed upon a purely logarithmic decay term. The form of this relationship can be written in terms of $P_r$ as[21]

$$P_r = A_1 \exp[-(t/\tau_0)^n] + [P_r(0) - A_2 \ln(t)], \qquad (1)$$

where $\tau_o$ is a characteristic relaxation time, $A_1$ is the non-equilibrium relaxation rate, $A_2$ is the relaxation rate in dynamical equilibrium, and $n$ is an exponent. Overall, the PMN-PT-5BT textured sample has slightly faster degradation than the PMN-PT-0BT random samples. To exclude the effect of Ag migration on the fatigue properties, samples with sputtered gold electrode were tested under the same condition as shown in Fig. 2(c). It can be seen that there is no difference between the Ag and Au electrode. To investigate the effect of BT template, the fatigue properties of textured PMN-PT with different concentration of template were measured. Fig. 2(d) shows the normalized remanant polarization as a function of number of cycles for PMN-PT-$x$BT ceramics. The fatigue resistance of textured ceramics first increases and then decreases with BT template content. This indicates that there are other factors such as grain size, BT-template clamping on the wall mobility, and grain anisotropy influencing the fatigue behavior.

The textured sample consists of random distribution of grain boundaries along with strong grain anisotropy like single crystals. Thus, to delineate the mechanism of fatigue, a systematic experiment is required to decouple the effect of polycrystalline microstructure and crystallographic anisotropy. In order to reveal the effect of cyclic electrical loading, micrographs were collected from the fractured surfaces of fatigue samples. As shown in Fig. 3(a), intergranular fracture was observed in the vicinity of the region about 200 $\mu$m below the electrodes, which indicates the weakening of the grain boundaries during the field cycling. It also indicates that the crack is originated from the grain boundary and not from the interface between matrix and template. To confirm that the fatigue mainly occured near the electrode, the piezoelectric constant ($d_{33}$), and dielectric constant ($\varepsilon_r$) of fresh, fatigued, and middle section (by polishing away the intergranular layer near the surface, Fatigue-M) of the fatigued sample were measured as shown in Fig. 3(b). It can be seen that the properties of middle section of fatigued sample were close to that of the fresh sample. Fig. 3(c) shows the XRD patterns of fresh and fatigued PMN-PT-5BT. After the electric field cycling, the Full-Width Half-Maximum (FWHM) of fatigued sample decreased, which could be due to the combination of residual strain and field induced phase transformation. After polishing away the porous (intergranular) layer near the surface, the XRD pattern of this middle (transgranular) section of fatigued sample showed similar FWHM as that of fresh sample. This is very interesting result indicating the strong influence of the surfacial layer on the overall macroscopic response and needs some discussion.

Nagata showed that the regions, where silver had diffused into the ceramic had much lower grain boundary strength than the bulk during the fracture.[15] Thus, one possible factor controlling the fatigue behavior could be the diffusion of silver along the grain boundaries due to low migration energy of silver under high electric field. Silver electro-migration can be viewed as the anodic dissolution of the metal, $Ag \rightarrow Ag^+ + e^{-1}$, transport of the $Ag^+$ ions through the electrolyte and, finally, reduction of the ion back to the metallic state at the cathode.[22] However, in our study, no difference in the fatigue behavior was obtained when using Ag or Au electrode (Fig. 2(c)). This excludes the possibility of silver diffusion and electro-migration. Another possible fatigue mechanism could be the domain-wall pinning by charged defect trapping at the domain boundaries. In this case, high temperature annealing should release the charged defects from the domain boundaries.[23] To investigate this hypothesis, dielectric constant as a function of temperature for fresh and fatigued PMN-PT-5BT ceramics (before and after annealing at 275 °C) was measured as shown in Fig. 3(d). After fatigue test, the dielectric constant decreased and the peaks of maximum dielectric constant were 10× lower. The ferroelectric-paraelectric phase transition temperature was increased from 162 °C to 178 °C. The peak of rhombohedral-tetragonal phase transition became obvious and the transition temperature increased. After annealing, the fatigued sample at 275 °C for 2 h, these two phase transition temperature decreased but did not fully recover to the fresh sample status. The frequency dispersion also decreased due to the partial removal of the charged defects such as oxygen vacancies. Therefore, we conclude that the presence of charged defect has significant effect on the fatigue behavior in textured PMN-PT ceramics. The fatigue initiates at the grain boundary because defects residing at the boundaries have lower potential energies compared with that in the bulk of the ferroelectrics.

The defect concentration in ferroelectric oxides can be evaluated by the electronic/ionic conductivity.[24] Fig. 4(a) shows the ac conductivity as a function of template content. With decrease of BT content ($x = 1$, 3, 5) in textured ceramics, the ac conductivity increases due to the difference in the defect density that are mainly located at the interfaces/boundaries. Therefore, complex impedance was employed to separate the individual contributions of grain interior and grain boundaries. As shown in Figs. 4(c) and 4(d), the impedance spectra displayed two semicircles, which are attributed to grain and grain boundary. The two semicircular arcs of the impedance spectrum can be expressed as equivalent circuit consisting of two parallel resistance-capacitance (R-C) circuit elements in series (the subscripts g and gb refer to grain (buck) and grain boundary). The values of grain (bulk) conductivity ($\sigma_g$) and grain boundary conductivity ($\sigma_{gb}$) obtained from these impedance spectra gave a linear Arrhenius plot as shown in Figs. 4(e) and 4(f). It can be seen that: (1) in case of $\sigma_g$, PMN-PT-5BT has higher activation energy and lower conductivity than PMN-PT-1BT. This is possible due to the large volume percentage of BT template residing inside the PMN-PT grains, which restricts the

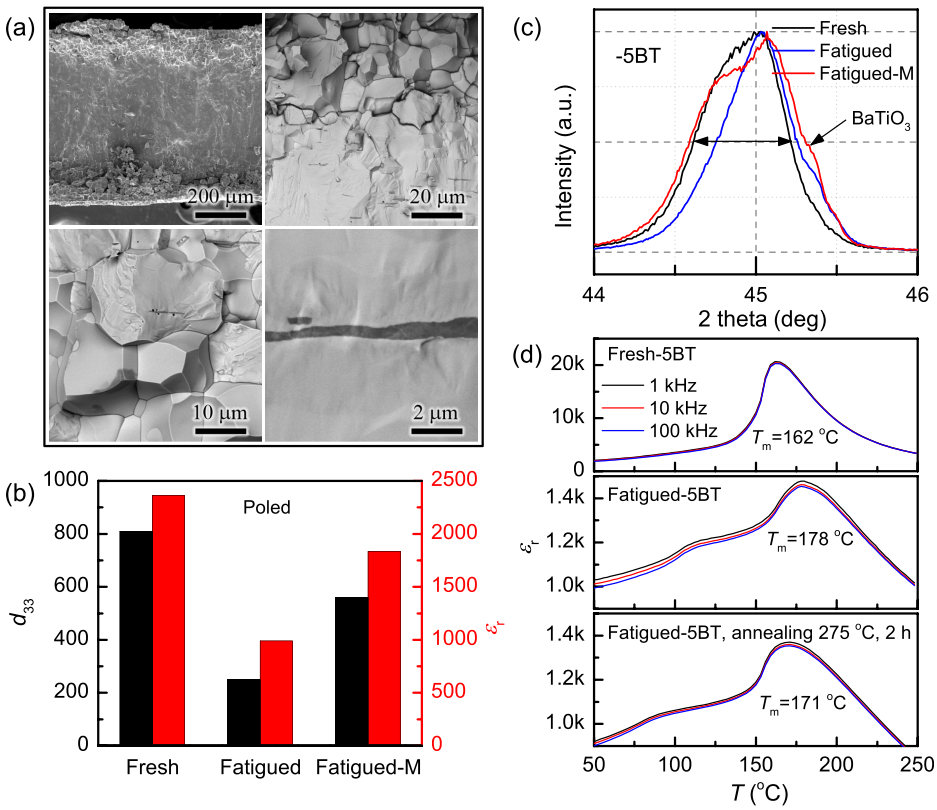


FIG. 3. (a) SEM images of textured PMN-PT-5BT fatigued sample (after $1.3 \times 10^6$ cycle) at different magnification; (b) piezoelectric ($d_{33}$) and dielectric constant ($\varepsilon_r$) of fresh, fatigued, and middle layer of fatigued PMN-PT-5BT sample; (c) XRD patterns of PMN-PT-5BT sample under different conditions, fresh, fatigued, and the middle (M) layer of fatigued sample; (d) dielectric constants as a function of temperature for fresh and fatigued PMN-PT-5BT samples.

migration of oxygen vacancies. (2) $\sigma_{gb}$ in PMN-PT-5BT and PMN-PT-1BT has similar activation energy, which indicates that the grain boundary has similar configuration. However, the grain boundary conductivity of PMN-PT-1BT is about 5 times higher than that of PMN-PT-5BT. From Fig. 4(b), the number of nucleation sites is decreased with decrease in BT template content ($x$), thus, the grain size ($d_g$) increases and the grain boundary area ($A_{gb}/V$) decreases, suggesting that the defect density around grain boundary in PMN-PT-1BT should be much larger than that in PMN-PT-5BT. Therefore, based on the consideration of defect density, higher template content will enhance the fatigue resistance because smaller grain size will result in lower defect concentration along the grain boundaries.

However, as shown in Fig. 4(b), the specific matrix/template interface area ($A_i$/V) increases with template content in textured PMN-PT ceramics. Increase in $A_i/V$ will deteriorate the fatigue behavior due to the clamping of the domain wall migration by the template particles. As evidenced by the polarization-electric field loops shown in Fig. 5(a), the polarization decreases, coercive field increases, and the squareness ($P_r/P_m$) of $P$-$E$ loops (Fig. 5(b)) decreases with increase of template content (samples with same texture degree). Thus, due to the opposing effect of template on the fatigue behavior in the textured ceramics (increase in template content reduces the defect density at grain boundaries but increases the domain wall pinning), the best fatigue properties are observed in PMN-PT-3BT as shown in Fig. 2(d). Piezoresponse force microscopy (PFM) images shown in Figs. 5(c) and 5(d) revealed that the domain size in textured ceramics is 10× smaller than that in random ceramics. Higher domain wall density in textured ceramics increases the domain wall motion, which facilitates the stress release during electric cycling. There is an optimum condition

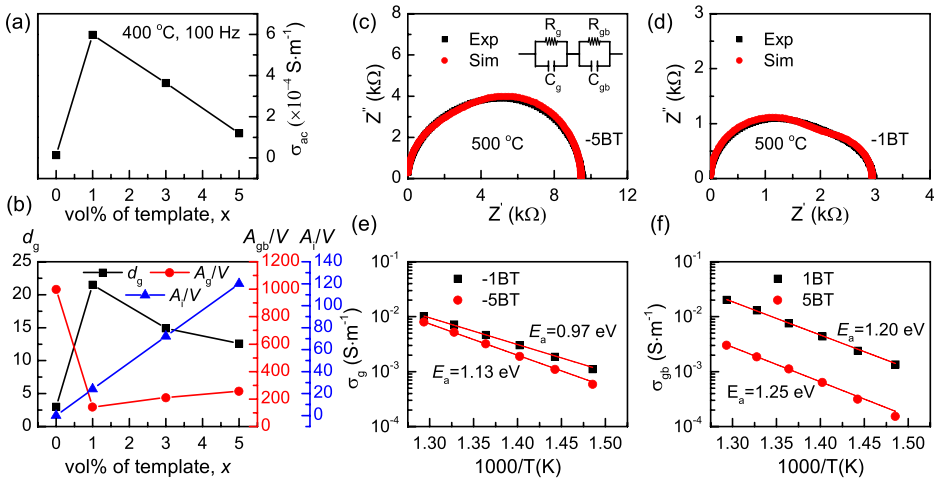


FIG. 4. AC conductivity ($\sigma_{ac}$) as a function of template content in PMN-PT-$x$BT textured ceramics at 400 °C, 100 Hz; (b) calculated grain size ($d_g$), specific grain boundary area ($A_{gb}/V$), and specific matrix/template interface area ($A_i$/V) as a function of template content ($x$, vol. %) in textured PMN-PT ceramics; experimental (Exp) and simulated (Sim) impedance spectra of (c) PMN-PT-5BT and (d) PMN-PT-1BT at 500 °C; (e) grain(bulk) conductivity ($\sigma_g$) and (f) grain boundary conductivity ($\sigma_{gb}$) versus inverse temperature ($1/T$) in PMN-PT-1BT and PMN-PT-5BT samples.

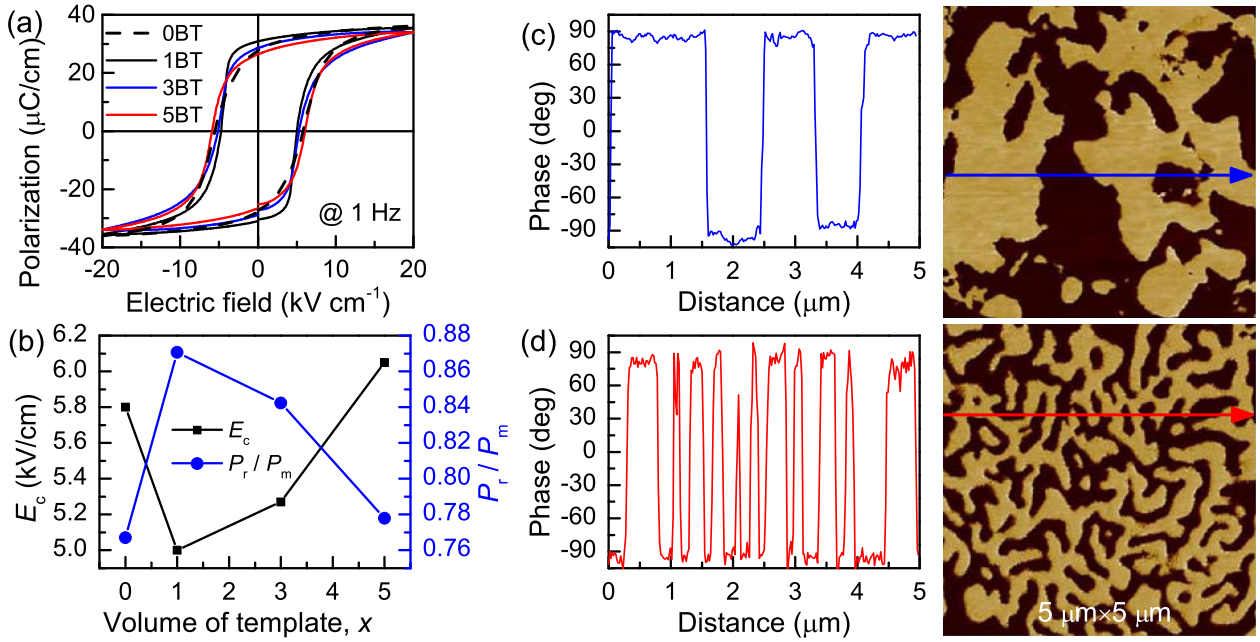


FIG. 5. (a) Polarization–electric field ($P$-$E$) loops and (b) coercive field ($E_c$) and $P_r/P_m$ for PMN-PT ceramics with different content of template. PFM images of (c) random and (d) 1 vol. % BT textured PMN-PT ceramics.

between the magnitude of domain wall mobility and template content, which in our study was found to be 3%. Even with the clamping effect from BT template, large grain size and higher conductivity, PMN-PT-3BT textured ceramics exhibited slower polarization degradation than the random PMN-PT-0BT ceramics in the first stage. Clearly in this case, the texturing influences the fatigue behavior because ⟨001⟩ crystal direction has a much better fatigue resistance. This result is consistent with that observed in other material systems such PMN-PT, PZN-PT, and PIN-PMN-PT single crystals.[13,14,22,25]

In summary, we found that ⟨001⟩ textured ceramics with 3% template content exhibits improved fatigue resistance due to the optimum balance between the defect density and domain mobility. As evident from the improved macroscopic $P$-$E$ loop squareness and PFM results, the role of charged defects and domain size have the controlling influence on the fatigue behavior. With increase of the template content from the optimum point, the clamping effect of the template on domain motion results in faster degradation of polarization.

The authors gratefully acknowledge the financial support from Office of Basic Energy Science, Department of Energy through Grant No. # DE-FG02-07ER46480. The authors would also like to thank the NSF I/UCRC: Center for Energy Harvesting Materials and Systems (CEHMS) for supporting the work on synthesis of textured piezoelectric materials.

[1]S. E. Park and T. R. Shrout, J. Appl. Phys. **82**, 1804 (1997).
[2]S. J. Zhang and F. Li, J. Appl. Phys. **111**, 031301 (2012).
[3]G. L. Messing, S. Trolier-McKinstry, E. M. Sabolsky, C. Duran, S. Kwon, B. Brahmaroutu, P. Park, H. Yilmaz, P. W. Rehrig, K. B. Eitel, E. Suvaci, M. Seabaugh, and K. S. Oh, Crit. Rev. Solid State Mater. Sci. **29**, 45 (2004).
[4]Y. K. Yan, Y. U. Wang, and S. Priya, Appl. Phys. Lett. **100**, 192905 (2012).
[5]Y. K. Yan, K. H. Cho, D. Maurya, A. Kumar, S. Kalinin, A. Khachaturyan, and S. Priya, Appl. Phys. Lett. **102**, 042903 (2013).
[6]D. C. Lupascu, *Fatigue in Ferroelectric Ceramics and Related Issues* (Springer, Berlin, New York, 2004).
[7]X. J. Lou, J. Appl. Phys. **105**, 024101 (2009).
[8]D. C. Lupascu and J. Rodel, Adv. Eng. Mater. **7**, 882 (2005).
[9]D. C. Lupascu and U. Rabe, Phys. Rev. Lett. **89**, 187601 (2002).
[10]J. F. Scott, *Ferroelectric Memories* (Springer, Berlin, New York, 2000).
[11]J. F. Scott, C. A. Araujo, B. M. Melnick, L. D. McMillan, and R. Zuleeg, J. Appl. Phys. **70**, 382 (1991).
[12]S. Pojprapai, J. Russell, H. Man, J. L. Jones, J. E. Daniels, and M. Hoffman, Acta Mater. **57**, 3932 (2009).
[13]F. Fang, W. Yang, and X. Luo, J. Appl. Phys. **106**, 094107 (2009).
[14]X. J. Lou, M. Zhang, S. A. T. Redfern, and J. F. Scott, Phys. Rev. Lett. **97**, 177601 (2006).
[15]H. Nagata, H. Haneda, I. Sakaguchi, T. Takenaka, and J. Tanaka, J. Ceram. Soc. Jpn. **105**, 805 (1997).
[16]S. J. Zhang, J. Luo, F. Li, R. J. Meyer, W. Hackenberger, and T. R. Shrout, Acta Mater. **58**, 3773 (2010).
[17]F. Fang, W. Yang, F. C. Zhang, and H. Qing, J. Mater. Res. **23**, 3387 (2008).
[18]M. Ozgul, S. Trolier-McKinstry, and C. A. Randall, J. Appl. Phys. **95**, 4296 (2004).
[19]K. Takemura, M. Ozgul, V. Bornand, S. Trolier-McKinstry, and C. A. Randall, J. Appl. Phys. **88**, 7272 (2000).
[20]Y. K. Yan, K. H. Cho, and S. Priya, J. Am. Ceram. Soc. **94**, 1784 (2011).
[21]S. Priya, J. Ryu, K. Uchino, and D. Viehland, Appl. Phys. Lett. **79**, 2624 (2001).
[22]N. J. Donnelly and C. A. Randall, J. Am. Ceram. Soc. **92**, 405 (2009).
[23]B. S. Li, G. R. Li, Q. R. Yin, Z. G. Zhu, A. L. Ding, and W. W. Cao, J. Phys. D **38**, 1107 (2005).
[24]N. V. Prasad, M. C. Sekhar, and G. S. Kumar, Ferroelectrics **366**, 55 (2008).
[25]J. K. Lee, J. Y. Yi, and K. S. Hong, J. Appl. Phys. **96**, 7471 (2004).